

An Assessment of the Best Estimate Thermal-Hydraulic Analysis Code CATHARE on CREARE Downcomer Experiment

Won-Pyo Chang, Jae-Hoon Lee, Dong-Su Kim, and Sung Ki Chae

Korea Atomic Energy Research Institute

(Received February 18, 1992)

CREARE Downcomer 실험에 대한 최적열수력 분석용 전산코드 CATHARE의 검증

장원표 · 이재훈 · 김동수 · 채성기

한국원자력연구소

(1992. 2. 18 접수)

Abstract

A 1/15-scale CREARE experiment, which simulates the thermal-hydraulic behavior in the reactor pressure vessel of a PWR during a hypothetical Loss Of Coolant Accident, has been analyzed using CATHARE code for the associated model assessment to represent the phenomenon. The key parameters examined in the CREARE experiment were known as ECC water injection rate, ECC water subcooling, system pressure, and steam flow rate coming out from the core bottom. The present CATHARE simulation, however, has been mainly focused on qualitative analysis of a countercurrent flow in the downcomer.

The discrepancy of the simulation results with the experimental data is considered arising primarily from an inadequate numerical representation as well as an interfacial friction model. Accordingly it is suggested from the sensitivity studies that either multidimensional approach or further examination of momentum equations at a junction near a volume element in CATHARE be necessary in order to represent the phenomenon more realistically.

요 약

가압경수로 최적 열수력 분석용 전산코드인 CATHARE의 모델 평가를 위하여 가압경수로의 가상 냉각재 상실사고시 원자로 용기내의 유동현상을 모의한 1/15 축소의 CREARE 실험을 모의 계산하였다. 이 실험에서 주요변수들은 비상노심 냉각재 주입량과 아냉정도 그리고 계통압력 및 노심에서 발생하는 증기유량이지만, 본 연구에서는 우선 Downcomer에서 역방향유동의 정성적 분석에 초점을 맞추었다.

모의 계산 결과와 실험 결과를 비교할 때 정량적인 값 뿐 아니라 변화의 경향에서도 차이가 나타난 것은 주로 적절하지 못한 일부의 수치해석 모델과 상간의 계면마찰 때문으로 판단된다. 따라서 매개변수적 민감도 분석을 통하여 CATHARE 전산코드의 'VOLUME'에 접한 접합점에서 운동량 보존방정식의 상세연구 혹은 다차원 분석을 통해서 이 경우의 물리적 현상을 보다 현실적으로 나타낼 수 있다는 결론을 얻었다.

1. Introduction

During the later stages of blowdown of a Pressurized Water Reactor (PWR) following a hypothetical Loss Of Coolant Accident (LOCA), steam generated by various sources flows up the annular downcomer on its way to the break as shown in Figure 1. At the same time, Emergency Core Cooling Water (ECCW) is injected through the cold legs. Since upflowing steam through annulus downcomer exerts drag force on the ECCW flowing down, ECCW may either penetrate into the lower plenum or directly bypass on the way to the break depending on momentum distribution within the upper plenum, interfacial friction in the downcomer, dimensional effect of downcomer and condensation [1].

The main purpose of CREARE experiment is to develop analytical and empirical tools which will contribute to best estimate and licensing prediction of larger scale lower plenum filling rate tests. However, it has not been possible to derive a reliable analysis of the countercurrent flow behavior using formal conservation equations. When the importance of lower plenum filling related with the countercurrent flow is reminded, an accurate prediction of physical phenomena occurring in downcomer is an essential subject to estimate core coolability. For this reason, overall adequacy as well as each physical model in CATHARE, French best estimate, 2-fluid, 6-equation, thermal-hydraulic code developed jointly by CEA, Framatome and EDF in France [3], contributing to represent such phenomena, should be examined for its reliable use.

In the simulation of 1/15-scale CREARE experiment, liquid delivered into the lower plenum through annulus downcomer has been estimated for given steam flow rates and the main parameters considered are ECCW subcooling, steam flow rate, water injection rate, and lower plenum pressure.

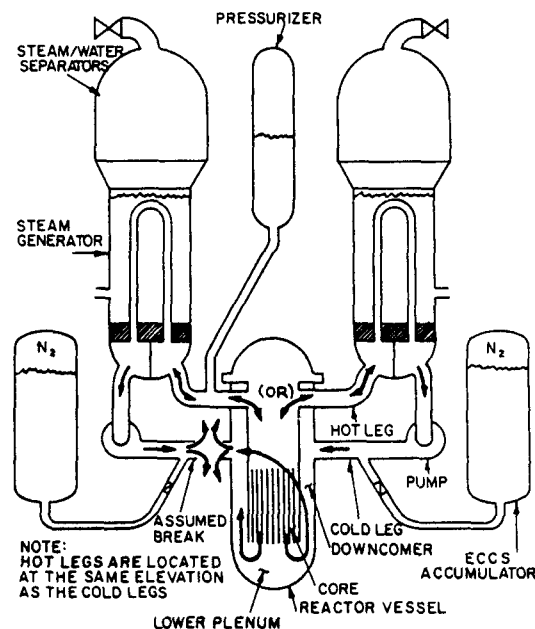


Fig. 1. Potential Flow Paths for a Cold Leg Break In a PWR [1]

2. Description of CREARE Experiment

The CREARE experiment had been conducted at CREARE Inc. in USA [4,5], and the basic component of the test facility is a 1/15-scale cylindrical model of a PWR reactor vessel. It has two gap size options (0.5 and 1.0 inches), two core barrel lengths (18 and 48 inches), and two vessel lengths, giving a total of six geometric combination. The system pressure is elevated either by increasing a flow resistance at break with valve closing or by controlling the pressure of containment-simulating separator vessel into which the broken leg flow discharges. Figure 2 shows an expected steam-water flow path during the countercurrent flow within vessel downcomer and Figure 3 illustrates the configuration of the vessel. The vessel has a multiloop injection configuration as shown in Figure 4. Each leg is linearly scaled, and hot and cold legs are interchangeable via inserts of the appropriate sizes. The vessel is a

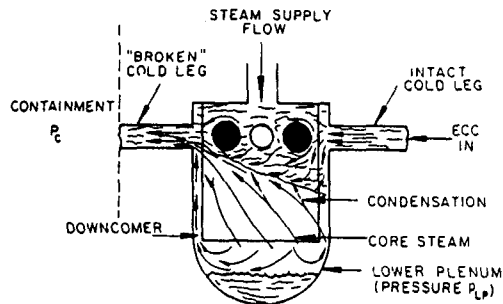


Fig. 2. Idealized Countercurrent Flow Situation

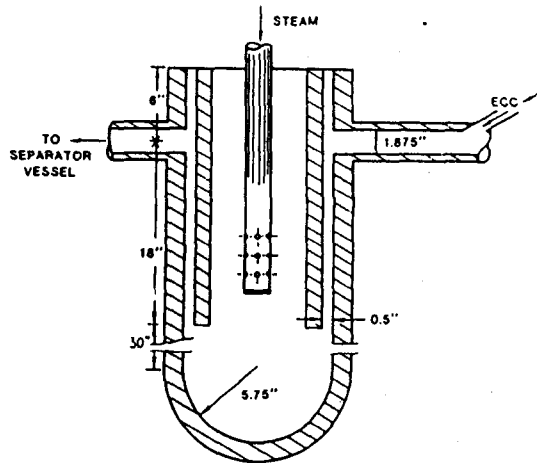


Fig. 3. Configuration of the Vessel

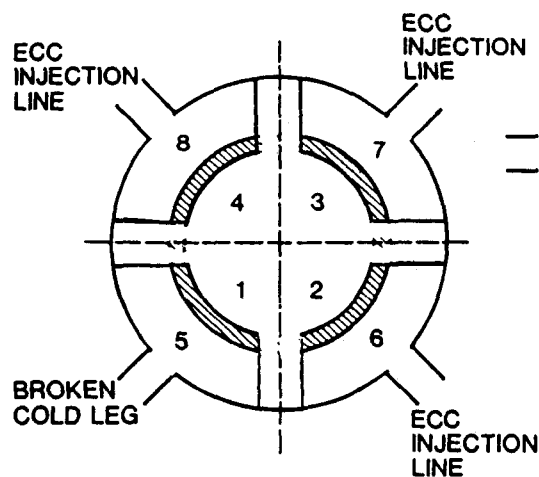


Fig. 4. Top View of 1/15-Scale CREARE Vessel

cylinder with an inside diameter of 11.5 inch thick wall. The core barrel is welded into the flange which forms the "upper head" of the vessel. Two core barrels are used to provide downcomer gap sizes of 0.5 and 1.0 inches. Each of the core barrels is 24 inches long, giving an 18 inch downcomer below the cold leg center line. Extensions are available to achieve 48 inch downcomer length as well.

System flow paths are illustrated in Figure 5. The ECC injection loop takes water from the ECCW tank and injects it into the vessel through the three simulated cold leg nozzles. Water from the vessel and separator is collected in drain tank and recycled. The heating system is also provided to preheat the metal surface. There is a cold water spray system in the separator vessel which is used to help control the simulated-containment pressure.

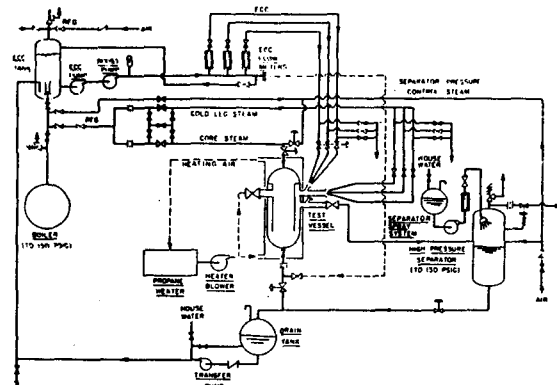


Fig. 5. Flow Schematic for CREARE 1/15-Scale High Pressure Cylindrical Vessel and Facility [2]

3. CATHARE Simulation

3.1. Nodalization of CREARE Experimental Facility

Figure 6 illustrates a schematic idealization of the major elements of CREARE experiment for

CATHARE simulation. An intact cold leg(COLDIN) weighted by 3 and a broken cold leg, whose diameters are two sizes, namely, 3" inner diameter for an enlarged break and 1.875" inner diameter for other cases, are all modelled by 'AXIAL'(PIPE) with 5 meshes and 10 meshes, respectively. Downcomer with 20 meshes also has been modelled by 'AXIAL' but with annulus geometry. The upper plenum and the lower plenum extended scale, consisting of a hemispheric geometry in the bottom and pipe geometry between core outlet and top of the hemisphere, are modelled as 'CAPACITY'(VOLUME) module. The nodalizations used in both saturated and subcooled ECCW injections are the same, however, in the subcooled ECCW injection heat structures not involved in the saturated ECCW injection are modelled in all the elements due to the temperature difference between wall and ECCW. ECCW is supplied at a constant temperature and flow rate so that 'BC3B' boundary condition is applied by specifying liquid velocity. Core steam supply from core outlet is modelled as 'BC3E' boundary condition which uses a mass flow rate in saturated ECCW injection. Finally the boundary condition at the end of the broken cold leg is given as a constant pressure provided by experimental data.

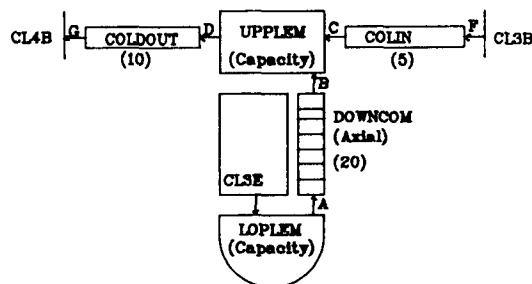


Fig. 6. Nodalization for 1/15-Scale CREARE Exp.

3.2. Simulation of Experiment

The simulation has been performed in accordance with the actual experiment. Steady state has

been made by supplying a saturated steam into the vessel first. 20 time steps of stabilized transient then begin with start of ECCW injection, reaching its steady state value with ramped rate for one second. This time period is arbitrarily chosen to avoid a numerical difficulty. The result of liquid delivery rate into the lower plenum(Q_{ld}) is usually picked up when the lower plenum is filled with water about 50% of its height. Since it is shown that a fairly constant rate has been established and usually CATHARE uses its maximum time step at this time. Finally, a transient is initiated by starting the steam injection, opening the break, and starting the ECCW injection at a given steam flow rate and a containment pressure. The transient is calculated until final steady state conditions are reached for some parameters shown in Figures 7-9. In Figure 7, ECCW injection reaches a steady state value for 1.0 second while core steam is constantly supplied at a given flow rate. The water delivery rate reaches a fairly steady state value after a short time of perturbation and drops to almost zero when the lower plenum is full. Consequently the lower plenum liquid level (Figure 8) and pressure(Figure 9) increase linearly due to an almost constant water delivery rate. These calculations confirm physical models in CATHARE are able to represent such a counter-

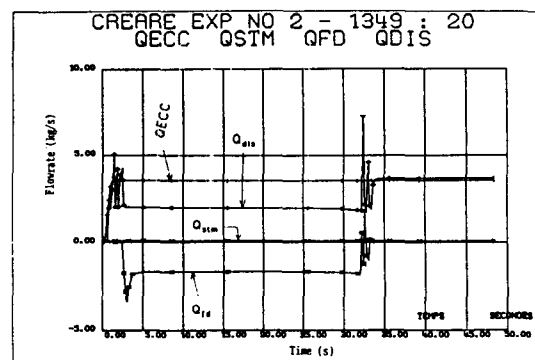


Fig. 7. Calculational Results for ECC Injection Rate, Steam Flowrate, Liquid Delivery Rate into the Lower Plenum and Break Flowrate

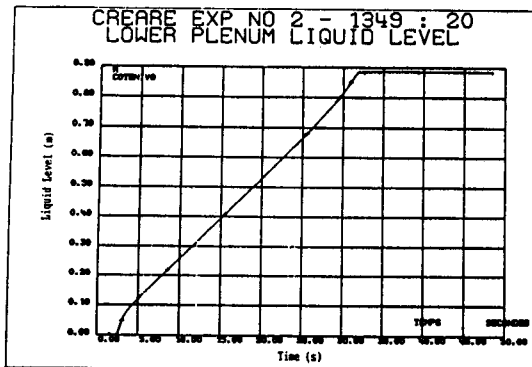


Fig. 8. Calculational Result for Lower Plenum Liquid Level

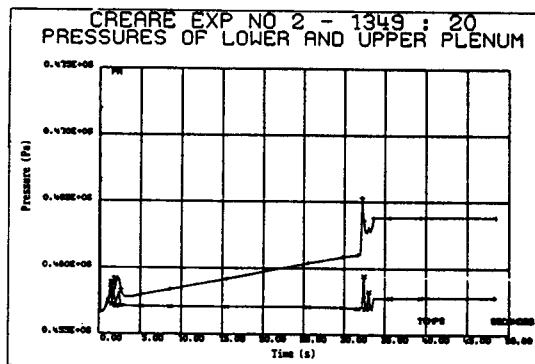


Fig. 9. Calculational Result for Pressures of Lower and Upper Plenum

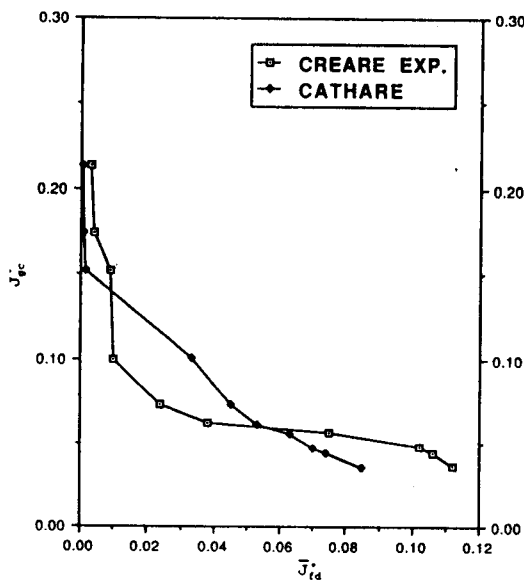


Fig. 10. Saturated ECC Flooding Curves at 2 bar

current flow expected in the downcomer geometry.

4. Results

4.1. Results for Saturated ECCW Injection

Calculational results with available saturated ECCW data[1] are plotted on Figure 10 and Figure 11 with experimental data. These results are corresponding to a system pressure of ~2 bars and 4~5 bars, respectively. In the plots dimensionless liquid delivery rate (\bar{J}_{ld}^*) and steam flow rate (\bar{J}_{gc}^*) which are defined as:

$$\bar{J}_{gc}^* = \frac{\rho_g \bar{J}_g^{1/2}}{[gW(\rho_f - \rho_g)]^{1/2}} \quad (1)$$

$$\bar{J}_{ld}^* = \frac{\rho_f \bar{J}_f^{1/2}}{[gW(\rho_f - \rho_g)]^{1/2}} \quad (2)$$

where;

\bar{J}_g, \bar{J}_f : superficial velocities of vapour and liquid

ρ_g, ρ_f : densities of vapour and liquid

g : gravitational acceleration

W : average annulus circumference(34.6")

These are parameters used for developing correlations in CREARE experiment[1]. Each point in the figures represents an experimental run at a given steam flow rate. Experimental data in Figure 10 show smooth decrease of \bar{J}_{ld}^* with steam flow rate while a rapid decrease of \bar{J}_{ld}^* is observed around lower steam flow ($\bar{J}_{gc}^* < \sim 0.7$), however, CATHARE predicts almost linear variation of \bar{J}_{ld}^* and thus liquid delivery rate into the lower plenum (Q_{ld}) is relatively overpredicted a near higher steam flow rate and underestimated at lower one. In addition, experimental data points corresponding to the lower steam flows tend to decrease suddenly near the complete delivery point, whose trend and magnitude are not predicted well by CATHARE. The calculated trend for the higher pressure in Figure 11 is similar to that of the lower pressure but a slight different trend is found in the

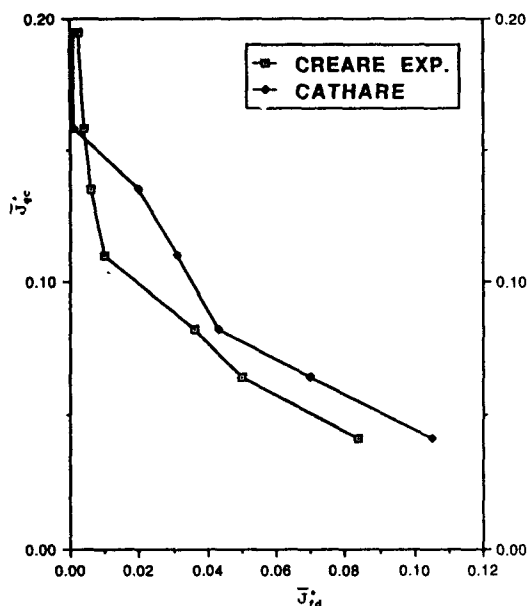


Fig. 11. Saturated ECC Flooding Curves at 4~5 Bars

experimental results from Figure 11 comparing with those from Figure 10. The non-dimensional parameters in eq. (1) and (2) are suspicious at this point. On the other hand, the discrepancies in Figure 11 seem to be smaller than those in Figure 10.

4.2. Results for Subcooled ECCW Injection

The calculated results are compared with experimental data in dimensionless form of steam upflow and delivered liquid flow in Figure 12 and 13. The agreement is satisfactory for the complete bypass point and for the high steam flow. However, the flow rate of liquid delivered to the lower plenum is underestimated in case of low steam flow rates. No high liquid flow has been calculated even with a very low steam flow rate. As very low steam flow was enough to keep back much water from entering the lower plenum, so the code seems to overpredict the interfacial friction for a low steam flow. Larger discrepancy was obtained for high subcooling (Figure 13) than for

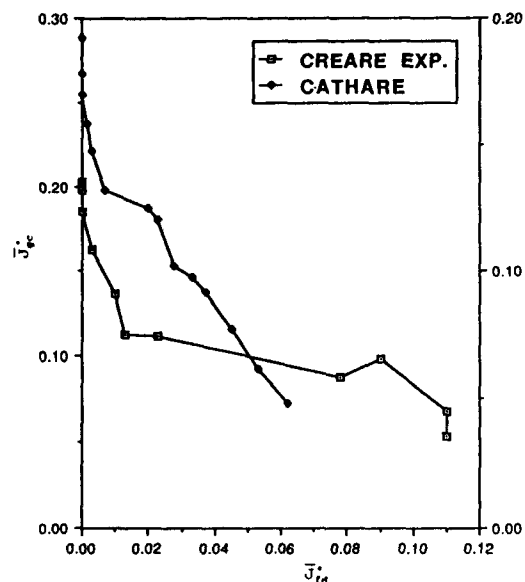


Fig. 12. 20°C Subcooled ECC Flooding Curves at 3 Bar

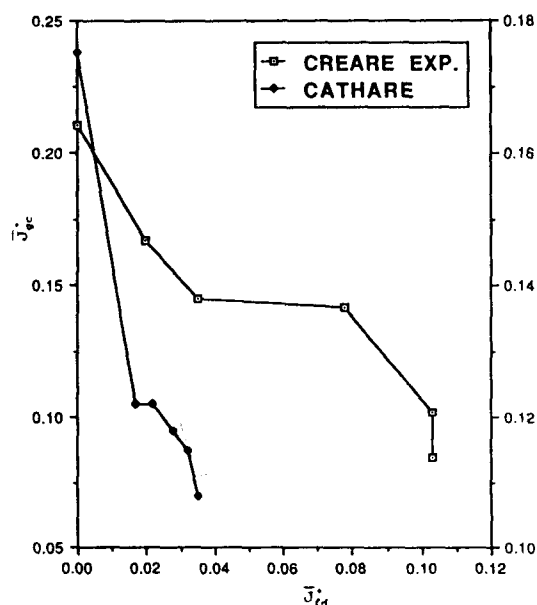


Fig. 13. 70°C Subcooled ECC Flooding Curves at 3 Bar

slightly subcooled (Figure 12) or saturated cases. Higher delivered liquid flow rates are expected with high subcooling than in slightly subcooled cases with the same injected steam and liquid flow

rates due to condensation, but the calculations give very small difference between these cases. This fact reveals underestimation of condensation effect.

5. Analysis

5.1. Sensitivity Study

As an effort to identify the main parameters affecting on a liquid delivery rate(Q_{ld}), the first attempt is a change of mesh size by dividing the downcomer into from 5 to 100 nodes as given in Table 1. Three runs, denoted by asterisks, result in different liquid delivery rates and different pressures. All Q_{ld} 's decrease with mesh numbers but they do not converge. On the other hand the change of the maximum time step does not affect on the liquid delivery rates(Table 2). For a quantitative investigation, those terms comprising a momentum conservation equation are evaluated

Table 2. Effect of Maximum Time Step on Q_{ld}

# of mesh	5	20	5	10
Max. Δt				
0.4 sec	2.079	1.343	0.260	2.003
0.8 sec	3.081	1.343	0.260	2.002
5.0 sec	3.080	1.341	0.261	2.001
10.0 sec	3.080	1.381	0.263	2.0

to examine for the relative importances on the results by comparing with each other. Three mesh numbers, namely, 5, 20 and 50 are chosen at 3 different axial positions along the downcomer, which are the adjacent node to the upper plenum junction, middle, and the node next to the lower plenum junction, respectively. The comparison of these results is given in Table 3. Important terms are usually those of gravitation, liquid acceleration and interfacial shear stress, whereas other terms are order of magnitude smaller than above terms. Among those terms the variation of liquid accel-

Table 1. Effect of Downcomer Mesh Size on Q_{ld}

# of mesh	Q_{ld} (Exp)	Exp. No	2-1360 3.444kg/s	1-1356 0.713kg/s	2-1362 0.113kg/s	*2-1349 1.665kg/s
5			3.080	1.976	0.263	2.365
10			3.863	1.634	0.148	2.0
20			2.600	1.381	bypassed	1.665
50			2.086	1.063	bypassed	1.333
100			1.829	0.9250	bypassed	1.207

Table 3. Effect of Mesh No on Each Term in Momentum Eq.

Term	Mesh No	Position	Near upper plenum			Middle			Near lower plenum		
			5	20	50	5	20	50	5	20	50
α_j			0.795	0.793	0.746	0.828	0.869	0.888	0.828	0.870	0.888
$(\rho_l - \rho_g)g$			9010	9102	9005	9005	9005	9005	9003	9001	8999
$\rho_l V_l(dV_l/dz)$			-3922	-5851	-6495	-1527	-873.2	-549	-905	14.6	427
$\tau_i(\alpha(1-\alpha))$			2563	2317	2311	2734	2418	2225	2860	2514	2302
$\rho_v V_v(dV_v/dz)$			4.8	72.1	238.0	-9.7	-1.1	-1.3	101.6	293	602
$(P_l/\alpha(1-\alpha))(d\alpha/dz)$			-37.0	-195.4	-522.5	-8.7	-5.5	-3.4	8.5	23.9	48.0
$(\tau_{wg}/\alpha) + (\tau_{wl}/(1-\alpha))$			-27.5	-10.0	-4.7	-51.8	-62.4	-68.0	-55.8	-67.4	-70.6
$(P_{wl}/\alpha(1-\alpha))$			-0.5	-2.7	-3.5	2.3	3.4	3.7	2.3	3.0	2.9

eration is particularly noticed at the adjacent node to the upper plenum. Slight changes of this term are also found at other points but the magnitudes are so small that they may not affect significantly on an overall momentum balance. Therefore, it is presumed that the inconsistency concerned with mesh number might result from the liquid acceleration term near the upper plenum. This fact could be confirmed by dividing downcomer with unequal mesh numbers instead of equal meshes. So the downcomer is divided into 8, 4, 8 and 8, 24, 8 meshes at near the upper plenum, middle, and near the lower plenum, respectively. The results are shown in Table 4 and 5 with equal meshes, i.e., 20 and 50. It is obvious from these results that the liquid delivery rate into the lower plenum is sensitive to mesh size near the upper plenum since the same mesh sizes near the upper plenum give consistent values for the liquid delivery rates regardless of total mesh numbers, however, only a different mesh size at this point gives another.

5.2. Analysis for 'CAPACITY' Module in CATHARE

A possible diagnosis for the observations caused by inconsistency existing in the momentum equations may be an inadequate numerical representation of the junction between a capacity module and an axial element. In CATHARE 'VOLUME'

Table 4. Effect of Mesh No Distribution on Q_{ld}

Mesh No	8.4.8.	8.24.8	20	50
Q_{ld}	1.345	1.346	1.665	1.333
Mesh size	0.0086	0.0086	0.0210	0.0084

module is presented by 2 sub-volume (Ω^+ , Ω^-) with a separation level Z_c as shown in Figure 14. For each sub-volume α (void Fraction), H_l (liquid enthalpy), H_g (gas enthalpy) are assumed uniform and calculated pressures (P) are located at the average elevation of each volume. However one pressure equation represents the total volume. The applied conservation equations are 2 mass balance equations, 2 energy balance equations, and 1 mass balance equation per noncondensable gas. Two momentum equations are considered at each junction while strongly simplified hydrostatic pressure equation ;

$$P^- - P^+ = (\alpha^- \rho_g^- + (1 - \alpha^-) \rho_l^-) \frac{Z_c}{2} + (\alpha^+ \rho_g^+ + (1 + \alpha^+) \rho_l^+) g \frac{Z_{max} - Z_c}{2} \quad (3)$$

is used to determine separation level between two sub-volumes. Among terms comprising momentum balance at the junction the finite-difference form of velocity derivatives dV/dZ , which is essential part in the representation of the accelerational pressure drop for a 'VOLUME-TUBE' type junction (Fig.15) has the following form :

Table 5. Upper Plenum (2% $Z_{max} = 0.0035m$)

Term	Mesh No	Position	Near upper plenum		Middle		Near Lower plenum	
			8.4.8	8.24.8	8.4.8	8.24.8	8.4.8	8.24.8
α_j			0.747	0.746	0.889	0.888	0.887	0.887
$(\rho_l - \rho_g)g$			9013	9013	9004	9006	9022	9022
$\rho_l V_l(dV_l/dZ)$			-6482	-6492	-370	-485	570	651
$\tau_l/\alpha(1-\alpha)$			2306	2299	2250	2227	2306	2303
$\rho_v V_v(dV_v/dZ)$			229	229	-2.9	-1.9	817	812
$(P_l/\alpha(1-\alpha))(d\alpha/dZ)$			-506	-506	-0.8	-2.8	61	62

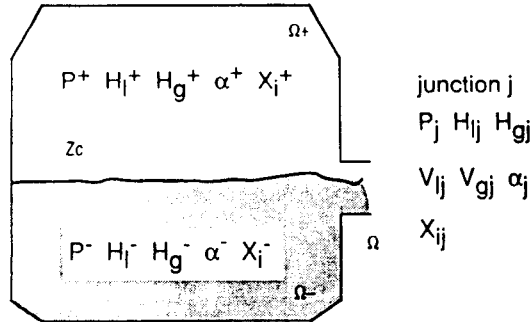


Fig. 14. Representation of 'VOLUME' Module in CATHARE

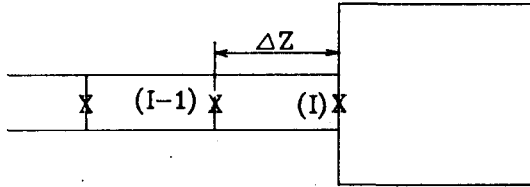


Fig. 15. Nodalization of 'AXIL-TUBE' Junction for Momentum Equation in CATHARE

$$\longrightarrow \text{for outflow case } \frac{V(I) - V(I-1)}{\Delta Z + 2\%H} \quad (4)$$

$$\longleftarrow \text{for inflow case } \frac{V(I)}{2 * (\Delta Z + 2\%H)} \quad (5)$$

where $2\%H = 2\%$ of maximum height

So the accelerational pressure drop depends on mesh size at 'VOLUME-TUBE' type junction and thus gives different velocity distribution along the downcomer as well as different liquid delivery rates. The main problem encountered due to mesh size really results from the dependence of the velocity derivatives for an inflow case on the axial mesh size. The ideal solution could be a multidimensional approach, however, another realistic approach would be to define a fixed velocity at a fixed point inside the volume. For a large volume zero velocity could be chosen as the fixed velocity with relatively large distance. Figure 16 gives the consistent results with different mesh numbers by choosing zero velocity at 25% of the maximum height [6].

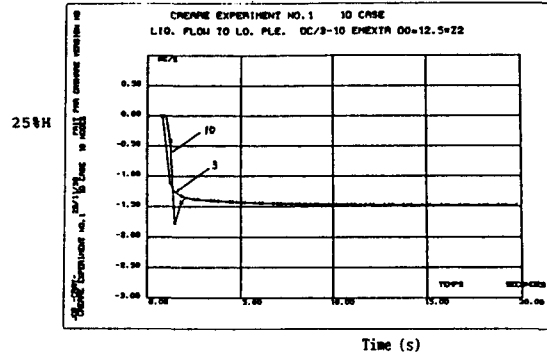


Fig. 16. Results for Liquid Delivery Rates for Mesh Number 3 and 10

5.3. Comparison with Experimental Data

Similar investigations are conducted to clarify the discrepancy observed in Figures 10 and 11. Since these results are obtained from saturated ECCW injections and thus mass or energy exchanges are considered relatively unimportant, a typical underestimated point at a low steam flow and an overpredicted one at a high steam flowrate are chosen to compare each term in momentum conservation equations. The calculated results are summarized in Table 6. Larger differences are found in both liquid acceleration and interfacial shear stress, however, the interfacial shear stress varies consistently at different positions. A relative contribution of the liquid acceleration to a pressure drop increases drastically at the adjacent node to the upper plenum when the steam flow is low, which leads a higher pressure drop resulting in a low downcomer liquid delivery.

Another point is that a higher void fraction is predicted for a higher steam flow rate and it remains almost constant along the downcomer while the void fraction for a lower steam flow near the upper plenum is reduced about 20% from that near the lower plenum. This fact represents steam flowing upward is more accelerated for the lower steam flow than for the higher one, probably due to the lower interfacial friction which affects posi-

Table 6. Effect of Steam Flow Rate on Each Term in Momentum Eq. ($Q_{\text{in}} = 3.6 \text{ kg/sec}$)

Position	Near upper plenum		Middle		Near lower plenum	
Exp. No Steam flow	2-1360	2-1358	-160	-1358	-1360	-1358
Terms	0.0391(kg/s)	0.1141(kg/s)				
$Q_{\text{fd}}(\text{Exp.})$	3.44(kg/s)	0.326(kg/s)				
$Q_{\text{fd}}(\text{CATHARE})$	2.60(kg/s)	0.918(kg/s)				
α_j	0.692	0.851	0.836	0.902	0.842	0.898
$(\rho_l - \rho_g)g$	9262	9248	9258	9242	9255	9238
$\rho_l V_l(dV_l/dZ)$	-7489	-3933	-1805	-194	-431	359
$\tau_{ij}/\alpha(1-\alpha)$	1016	4134	050	4083	1138	4193
$\rho_v V_v(dV_v/dZ)$	39.8	85.7	-2.13	-2.62	132.4	568.9

tively on the steam flow. Since the term representing the interfacial friction is not affected by the void fraction so sensitively, the interfacial friction is considered underestimated comparing with the acceleration term for a larger relative velocity, which corresponds to the case of the lower steam flow rate. According to the reference [7], the interfacial shear stress is completely based on Wallis drift flux model and somehow simplified due to numerical reason.

Therefore the dominant discrepancy seems to come from unrealistic representation on liquid acceleration near the upper plenum because downward liquid flow depends usually on the momentum distribution at each junction in the upper plenum. The volume average velocity and the length which characterizes the velocity, which comprise the eq. (5), are those of the key parameters to be improved in the acceleration term. The interfacial shear stress is also to be examined on a separated effect test with different relative velocities for a better simulation including further sensitivity studies.

6. Conclusions

Based on the calculational results, following conclusions are obtained:

1. CATHARE does not predict the experimental trend and magnitude well, specially for the lower pressure (~2 bars), which results in the under- and over-prediction of the liquid delivery rates (Q_{fd}) at lower and higher steam flow rates, respectively. The code also under-estimates the condensation phenomena in highly subcooled case.
2. The numerical modelling of the CATHARE at 'VOLUME-TUBE' junction associated with the volume average velocity and the corresponding characteristic length in eq.(5) should be improved through both numerical study and experiment, since the effect of the liquid acceleration near the upper plenum is regarded as a dominant factor affecting on the liquid delivery rate.
3. The analysis of discrepancy observed at a low system pressure (~2 bars) shows the under-estimation of the interfacial shear stress comparing with the acceleration term for a larger relative phasic velocity. Since the interfacial shear stress is mostly composed of experimentally determined correlation, it is suggested that the correlations be fitted on the CREARE experiment first and then they would be validated against a different scale experiment.
4. Multi-dimensional analysis would be another option to overcome problems related with momentum distribution in the upper plenum in order to analyze ECC injection into the core.
5. Quantitative sensitivity studies associated with physical models are almost impossible with in

a few years because most of such models are usually based on the experimental correlations, for which properly designed experimental facility does not exist in this country. Accordingly, an alternative approach would be studying the experiments and modellings obtained from other countries for a while until environment for such studies is matured enough.

6. The trends in Figure 10 and that in Figure 11 are different. This fact leads to the suspicion of either the inconsistencies of the experiments or inadequate representation of the non-dimensional parameters in eq. (1) and (2). It also requires another experiments with a different system pressure and the additional numerical tests in the future.

7. Acknowledgements

Authors give a heartfelt appreciation to CATHARE team staffs for supporting to use CATHARE code. Close cooperation with Z. Hozer from Hungary for the calculations of sub-cooled ECCW injection experiments and discussions on sensitivity studies, is also remarked.

References

1. P.H. Rothe and C.J. Crawley, "Scaling of Pressure and Subcooling for Countercurrent Flow", NUREG/CR-0464, TN-285, Oct. 1978
2. M. Pellissier and P. Chetatelard, "Remplissage CREARE 1/15 : Reconstitution d'essais et Extrapolation a l'e'chelle 1 avec les Codes CATHARE et TRAC", SETH/LEML/89-97, Oct. 1989
3. F. Barre and M. Benard, "The CATHARE Code Strategy and Assessment", Nuclear Engineering and Design, Vol.124, No.3, 1990
4. J.A. Block and C.J. Crawley, "Countercurrent Flow, Coupled Cold Leg Steam, and Transient Steam Flow Test at 1/15-Scale", CREARE TN-247, Sep. 1976
5. C.J. Crawley, J.A. Block and C.N. Cary, "Downcomer Effect in a 1/15-Scale PWR Geometry. Experimental Data Report", NUREG-2081, NRC-2, May 1977
6. Z. Hozer, "Some Remarks on the Discretization of the Momentum Equations for 'VOLUME-TUBE' Type Junctions", Presentation of CATHARE Technical Meeting at CENG, Dec. 1990
7. D. Bestion, "Description Generale Des Lois Physiques Du Module De Base", SETH/LEML-EM/89-190